Accepted for Publication, Published online October 31, 2016; doi:10.4269/ajtmh.16-0585.
The latest version is at http://ajtmh.org/cgi/doi/10.4269/ajtmh.16-0585

Isolation of Coronavirus NL63 from Blood from Children in Rural Haiti: Phylogenetic Similarities with Recent Isolates from Malaysia

Valery Madsen Beau De Rochars,[1,2] John Lednicky,[1,3] Sarah White,[1,3] Julia Loeb,[1,3] Maha A. Elbadry,[1,3] Taina Telisma,[1,4] Sonese Chavannes,[1,4] Marie Gina Anilis,[1,4] Eleonora Cella,[1,5,6] Massimo Ciccozzi,[6] Bernard A. Okech,[1,3] Marco Salemi,[1,5] and J. Glenn Morris Jr.[1,7]*

[1]*Emerging Pathogens Institute, University of Florida, Gainesville, Florida;* [2]*Department of Health Services Research, Management and Policy, College of Public Health and Health Professions, University of Florida, Gainesville, Florida;* [3]*Department of Environmental and Global Health, College of Public Health and Health Professions, University of Florida, Gainesville, Florida;* [4]*Christianville Foundation, School Clinic, Gressier, Haiti;* [5]*Department of Pathology, Immunology and Laboratory Sciences, College of Medicine, University of Florida, Gainesville, Florida;* [6]*Department of Infectious Parasitic and Immunomediated Diseases, Reference Centre on Phylogeny, Molecular Epidemiology and Microbial Evolution (FEMEM)/Epidemiology Unit, Istituto Superiore di Sanita, Rome, Italy;*[7]*Department of Medicine, College of Medicine, University of Florida, Gainesville, Florida*

* Address correspondence to J. Glenn Morris Jr., Emerging Pathogens Institute, University of Florida, 2055 Mowry Road, P.O. Box 100009, Gainesville, FL 32610-0009. E-mail: jgmorris@epi.ufl.edu

Abstract.

Human coronavirus (HCoV) NL63 is recognized as a common cause of upper respiratory infections and influenza-like illness. In screening children with acute undifferentiated febrile illness in a school cohort in rural Haiti, we identified HCoV-NL63 in blood samples from four children. Cases clustered over an 11-day period; children did not have respiratory symptoms, but two had gastrointestinal complaints. On phylogenetic analysis, the Haitian HCoV-NL63 strains cluster together in a highly supported monophyletic clade linked most closely with recently reported strains from Malaysia; two respiratory HCoV-NL63 strains identified in north Florida in the same general period form a separate clade, albeit again with close linkages with the Malaysian strains. Our data highlight the variety of presentations that may be seen with HCoV-NL63, and underscore the apparent ease with which CoV strains move among countries, with our data consistent with recurrent introduction of strains into the Caribbean (Haiti and Florida) from Asia.

Human coronaviruses (HCoVs) are being recognized with increasing frequency globally as a cause of human respiratory infections.[1–8] Strains are also associated with infections in animals, with current data suggesting that bats are a primary reservoir and point of origin for HCoVs.[9,10] Initially described in the 1960s, interest in the coronaviruses increased substantially in the early 2000 with the emergence of severe acute respiratory syndrome (SARS),[11] followed by the Middle East respiratory syndrome (MERS) in 2012.[12] Other than SARS and MERS, which have tended to occur in more delimited epidemics, four coronaviruses are currently recognized as being endemic in human populations: HCoV-229E, HCoV-OC43, HCoV-NL63, and HCoV-HKU1.[1–8]

Our group works closely with the school clinic that serves four schools operated by the Christianville Foundation in the Gressier/Leogane region of Haiti, some 20 miles west of Port-au-Prince. The schools have a total of approximately 1,250 students, from prekindergarten to grade 12.[13] Because of our interest in monitoring arboviral transmission within this population,

we have protocols in place for the collection of diagnostic blood samples from children presenting to the school clinic with acute undifferentiated febrile illness (i.e., febrile illness with no localizing signs, such as would be expected with pneumonia, upper respiratory infections, urinary tract infections). The protocol for sample collection was approved by the University of Florida Institutional Review Board (IRB) and the Haitian National IRB, and written parental informed consent was obtained from parents or guardians of all study participants.

CASE REPORTS

Between May 2014 and February 2015, blood samples were obtained at the school clinic from a total of 177 children who met criteria for the diagnosis of acute undifferentiated febrile illness. HCoV-NL63 was identified in samples from four case patients seen between January 16 and January 27, 2015. Ages ranged from 3 to 10 years (mean 6 years). All presented with subjective symptoms of fever, although only two were febrile when examined (39°C and 38.5°C, respectively). Two complained of headache, whereas two complained of "abdominal flu." In keeping with the criteria for enrollment in the study, no respiratory symptoms or symptoms consistent with croup were reported. Routine stool cultures and examination for ova and parasites were performed on stool samples from all four children, as previously described[13]: *Giardia* was identified in the stool sample of one of the children with abdominal complaints, and *Blastocystis* was identified in one of the children with no gastrointestinal (GI) complaints. No bacterial pathogens were identified on stool culture. Malaria screens on all four children were negative. In all instances, illness was mild and self-limited, and children recovered without sequelae.

Plasma samples were cultured using cell lines and conditions as previously described,[14,15] and as reported in detail in the Supplemental Information that accompanies this publication. In brief, aliquots of plasma (25–100 μL) from each patient were inoculated in duplicate into five different cell lines (A549, LLC-MK2, MDCK, MRC5, and Vero E6). Cell cultures from each of the four patients displayed cytopathic effects (CPEs) that were clearly different from those observed in cells in which alpha-, flavi-, and other viruses were isolated (Figure 1). The CPE were most obvious in LLC-MK2 cells and less so in Vero E6 incubated at either 33°C or 37°C.

Primary screens of spent culture from these cell cultures by reverse transcription polymerase chain reaction (RT-PCR) were negative for arena-, alpha-, entero-, and flavivirus viral genomic RNAs (vRNAs); however, they were positive for HCoV-NL63 using the GenMark eSensor XT-8 RVP system (eSensor RVP; GenMark Diagnostics, Inc., Carlsbad, CA). The agent isolated in these cultures was subsequently confirmed as HCoV-NL63 by RT-PCR and sequencing of the amplicons and the virus genome. Similar methods were used to obtain sequence data for HCoV-NL63 from two positive respiratory samples collected in July and September 2015, respectively, at University of Florida Health/Shands Hospital in Gainesville, FL. GenBank accession numbers: HCoV-NL63/Haiti: KT266906; KX179494- KX179499. HCoV-NL63/Florida: KT381875.1; KU521535.1.

A multiple sequence alignment was assembled including 192 HCoV-NL63 spike gene region reference sequences, downloaded from NCBI (see Supplemental Table 1 for details about the reference sequences), plus the four Haitian sequences and the two sequences from University of Florida Health. The locations of the reference sequences considered for the analysis were Belgium, China, Ghana, Hong Kong, Japan, Malaysia, Netherlands, Sweden, Thailand, and the United States. The evolutionary model was chosen as the best-fitting nucleotide substitution

model in accordance with the results of the hierarchical likelihood ratio test implemented with the Modeltest software version 3.7.[16] See supplemental Information for a complete description of phylogenetic methods.

Bayesian factor (BF) analysis showed that a significant better fit for the relaxed rather than the strict molecular clock model (LnBF > 15 in favor of the former). Under the relaxed clock, the BF analysis also showed that the nonparametric Bayesian skyline plot was the best-fitting demographic model (LnBF > 53 for each comparison). The estimated mean evolutionary rate was 7.02×10^{-4} substitutions/site/year (95% high posterior density [HPD] 3.97×10^{-4}–1.09×10^{-3}). The Maximum Clade Credibility tree shows three main supported clades (Figure 2) with no particular geographic structure, although it is clear that the older lineages, close to the root of the tree are from United States with a most recent common ancestor dating back to the mid-1970s (a tree with reference labels is provided in Supplemental Figure 1).

The four new Haitian isolates belonged to genotype C and clustered within a well-supported ($P > 0.95$) sub-clade with a most recent common ancestor dating back to 2013 (95% high posterior density intervals 2012–2014). The two Florida sequences also clustered with genotype C sequences and formed a separate but highly supported sub-clade ($P > 0.95$), with a most recent common ancestor dating back to 2014 (95% HPD intervals 2013.5–2014.5). The Haitian and Florida isolates and a strain from Malaysia are part of a larger sub-clade branching off independently from several genotype C Malaysian sequences,[17] which would suggest an Asian origin for the new strains, although the sub-clade does not have strong statistical support ($P < 0.9$). Overall, the data are consistent with at least two recent and independent introductions of HCoV-NL63 virus in the region (one in Haiti, one in north Florida), possibly originating from east Asia.

DISCUSSION

HCoV-NL63 is widely distributed in human populations, and has been isolated from patients with symptoms ranging from those of a mild "common cold" to influenza-like illness, and, rarely, pneumonia and more severe lower respiratory infections.[1–8] Cases tend to cluster, often in winter/late winter months in temperate areas, although there is a wide variation in seasonality in different parts of the world. In comparison to the other common HCoV groups, NL63 has been reported as the most common cause of croup in infants < 6 months of age.[7] It is also commonly seen as a coinfection with other known pathogenic viruses (38% of total cases in one study were infected with two or more viruses[7]), and, in a study in Ghana, which compared children with respiratory symptoms with control children without such symptoms, HCoV-NL63 was significantly more common among control children than case children (8.5% versus 6.8%, P 0.022).[3] HCoV (including HCoV-NL63) have also been identified in stool samples from children with acute gastroenteritis; however, 82% of patients from whom HCoV were isolated also had either norovirus or rotavirus in the stool sample.[18] Taken together, these data paint a picture of a widely distributed virus, present in the respiratory and GI tract, with uncertain pathogenicity, possibly due to inherently low virulence and/or the impact of high levels of prior immunity in the general population.

In this study, we isolated HCoV-NL63 from a small cluster of children with febrile illness, without respiratory symptoms, in January in rural Haiti. As our primary goal was to screen for arboviruses, we specifically excluded children with respiratory symptoms from sample collection, so we cannot be certain how many of this latter group might also have been infected

with/carrying HCoV-NL63. What was unexpected was the isolation of this specific coronavirus group from blood, which, to our knowledge, has not been previously reported. However, viremia is not totally unexpected: HCoV-NL63 is capable of infecting human kidney cells in tissue culture[19] by using the same cell receptor (ACE2 receptor) as SARS-CoV, which causes systemic illness, and is shed in respiratory secretions, urine, and stools, with presumptive hematogenous spread. The clinical significance of the viremia in our specific cases is uncertain. All case patients were febrile, and two had GI complaints (although one of the two with GI complaints also had *Giardia* on stool examination). Our findings indicate that viremia with HCoV-NL63 does occur, and raise the possibility that it can cause a mild febrile illness in otherwise healthy children, without respiratory manifestations, but, possibly, with diarrhea.

At a phylogenetic level, our Haitian isolates were most closely linked with isolates from Malaysia. We also sequenced two HCoV-NL63 isolates from respiratory samples at University of Florida Health in Gainesville: they clustered together within a separate monophyletic clade, with a separate link back to Malaysian strains. These findings underscore the apparent ease with which coronavirus strains can spread at a global level, findings in keeping with the observed continental jumps of both SARS-CoV and MERS-CoV.[20]

Received July 19, 2016.

Accepted for publication September 16, 2016.

Note: Supplemental information, table, and figures appear at www.ajtmh.org.

Authors' addresses: Valery M. Beau de Rochars, Emerging Pathogens Institute, University of Florida, Gainesville, Florida and Department of Health Services Research, Management and Policy, University of Florida, Gainesville, FL, E-mail: madsenbeau@phhp.ufl.edu. John Lednicky, Sarah White, Julia Loeb, Maha A. Elbadry, and Bernard A. Okech, Emerging Pathogens Institute, University of Florida, Gainesville, FL and Department of Environmental and Global Health, College of Public Health and Health Professions, University of Florida, Gainesville, FL, E-mails: jlednicky@phhp.ufl.edu, sek0005@ufl.edu, jloeb@phhp.ufl.edu, elbadrym@ufl.edu, and bokech@ufl.edu. Taina Telisma, Sonese Chavannes, and Marie Gina Anilis, Emerging *Pathogens Institute, University* of Florida, Gainesville, Florida and Christianville Foundation, School Clinic, Gressier, Haiti, E-mails: tainaquisqueya@gmail.com, chavannessonse@yahoo.fr, and mariegina_anilis@yahoo.fr. Eleonora Cella, Emerging Pathogens Institute, University of Florida, Gainesville, FL, Department of Pathology, Immunology and Laboratory Sciences, College of Medicine, University of Florida, Gainesville, Florida, and Department of Infectious Parasitic and Immunomediated Diseases, Reference Centre on Phylogeny, Molecular Epidemiology and Microbial Evolution (FEMEM)/Epidemiology Unit, Instituto Superiore de Sanita, Rome, Italy, E-mail: eleonora.cella@yahoo.it. Massinno Ciccozzi, Department of Infectious Parasitic and Immunomediated Diseases, Reference Centre on Phylogeny, Molecular Epidemiology and Microbial Evolution (FEMEM)/Epidemiology Unit, Istituto Superiore di Sanita, Rome, Lazio, Italy, E-mail: ciccozzi@iss.it. Marco Salemi, Emerging Pathogens Institute, University of Florida, Gainesville, FL, and Department of Pathology, Immunology and Laboratory Sciences, College of Medicine, University of Florida, Gainesville, FL, E-mail: salemi@pathology.ufl.edu. J. Glenn Morris Jr., Emerging Pathogens Institute, University of Florida, Gainesville, FL, and Department of Medicine, College of Medicine, University of Florida, Gainesville, FL, E-mail: jgmorris@epi.ufl.edu.

REFERENCES

<jrn>1. Berry M, Gamieldien J, Felding BC, 2015. Identification of new respiratory viruses in the new millennium. *Viruses 5:* 996–1019.</jrn>

<jrn>2. Yip CCY, Lam CSF, Luk HKH, Wong EYM, Lee RA, So L-Y, Chan K-H, Cheng ACC, Yuen K-Y, Woo PCY, Lau SKP, 2016. A six-year descriptive epidemiological study of human coronavirus infections in hospitalized patients in Hong Kong. *Virol Sin 31:* 41–48.</jrn>

<jrn>3. Owusu M, Annan A, Corman VM, Larbi R, Anti P, Drexler JF, Agbenyega O, Adu-Sarkodie Y, Drosten C, 2014. Human coronavirus associated with upper respiratory tract infections in three rural areas of Ghana. *PLoS One 9:* e99782.</jrn>

<jrn>4. Matoba Y, Abiko C, Ikeda T, Aoki Y, Suzuki Y, Yahagi K, Matsuzaki Y, Itagaki T, Katsushima F, Katsuchima Y, Mizuta K, 2015. Detection of human coronavirus 229E, HKU1, NL 63, and OC43. *Jpn J Infect Dis 68:* 138–141.</jrn>

<jrn>5. Huang S-H, Su M-C, Tien N, Huang C-J, Lan Y-C, Lin C-S, Chen C-H, Lin C-W, 2015. Epidemiology of human coronavirus NL63 infection among hospitalized patients with pneumonia in Taiwan. *J Microbiol Immunol Infect*. doi: 10.1016/j.jmii.2015.10.008.</jrn>

<jrn>6. Razuri JH, Malecki M, Tinoco Y, Ortiz E, Guezala MC, Romero C, Estela A, Brena P, Morales M-L, Reaves EJ, Gomez J, Uyeki TM, Widdowson M-A, Azziz-Baumgartner, Bausach DG, Schildgen V, Schildgen O, MontgomeryJM, 2015. Human coronavirus-associated influenza-like illness in the community setting in Peru. *Am J Trop Med Hyg 93:* 1138–1140.</jrn>

<jrn>7. Lee J, Storch GA, 2014. Characterization of human coronavirus OC43 and human coronavirus NL63 infections among hospitalized children <5 years of age. *Pediatr Infect Dis J 33:* 814–820.</jrn>

<jrn>8. Trombetta H, Faggion HZ, Leotte J, Nogueira MB, Vidal LRR, Raboni SM, 2016. Human coronavirus and severe acute respiratory infection in southern Brazil. *Pathog Glob Health 110:* 113–118.</jrn>

<jrn>9. Hu B, Ge X, Wang L-F, Shi Z, 2015. Bat origin of human coronaviruses. *Virol J 12:* 221.</jrn>

<jrn>10. Huynh J, Li S, Yount B, Smith A, Sturges L, Olsen JC, Nagel J, Johnson JB, Agnihothram S, Gates JE, Frieman MB, Baric RS, Donaldson EF, 2012. Evidence supporting a zoonotic origin of human coronavirus strain NL63. *J Virol 86:* 12816–12825.</jrn>

<jrn>11. Ksiazek TG, Erdman D, Goldsmith CS, Zaki SR, Peret T, Emery S, Tong S, Urbani C, Comer JA, Lim W, Rollin PE, Dowell SF, Ling AE, Humphrey CD, Shieh WJ, Guarner J, Paddock CD, Rota P, Fields B, DeRisi J, Yang JY, Cox N, Hughes JM, LeDuc JW, Bellini WJ, Anderson LJ; SARS Working Group, 2003. A novel coronavirus associated with severe acute respiratory syndrome. *N Engl J Med 348:* 1953–1966.</jrn>

<jrn>12. de Groot RJ, Baker SC, Baric RS, Brown CS, Drosten C, Enjuances L, Rouchier RAM, Galiano M, Gorbalenya AE, Memish ZA, Perlman S, Poon LLM, Snijder EJ, Stephens GM, Woo PCY, Zaki AM, Zambon M, Ziebuhr J, 2013. Middle east respiratory syndrome coronavirus (MERS-CoV): announcement of the Coronavirus Study Group. *J Virol 87:* 7790–7792.</jrn>

<jrn>13. Beau De Rochars VEM, Alam MT, Telisma T, Masse R, Chavannes S, Anilis MG, Guillaume JH, Gelin G, Kirkpatrick EL, Desormeaux A-M, Okech BA, Weppelmann TA, Rashid M, Karst S, Johnson JA, Ali A, Morris JG Jr, 2015. Spectrum of outpatient illness in a school-based cohort in Haiti, with a focus on diarrheal pathogens. *Am J Trop Med Hyg 92:* 752–757.</jrn>

<jrn>14. Lednicky J, Beau de Rochars VM, ElBadry M, Loeb J, Telisma T, Chavannes S, Anilis G, Cella E, Ciccozzi M, Rashid M, Okech B, Salemi M, Morris JG Jr, 2016. Zika virus outbreak in Haiti in 2014: molecular and clinical data. *PLoS Negl Trop Dis 10:* e0004687.</jrn>

<jrn>15. El Badry M, Lednicky J, Cella E, Telisma T, Chavannes S, Loeb J, Ciccozzi M, Okech B, Beau De Rochars VM, Salemi M, Morris JG Jr, 2016. Isolation of an entervirus D68 from blood of a child with pneumonia in rural Haiti: close phylogenetic linkage with New York strain. *Ped Infect Dis J 35:* 1048–1050..</jrn>

<jrn>16. Posada D, Buckley TR, 2004. Model selection and model averaging in phylogenetics: advantages of akaike information criterion and bayesian approaches over likelihood ratio tests. *Syst Biol 53:* 793–808.</jrn>

<jrn>17. Al-Khannaq MN, Ng KT, Oong XY, Pang YK, Takebe Y, Chook JB, Hanafi NS, Kamarulzaman A, Tee KK, 2016. Diversity and evolutionary histories of human coronaviruses NL63 and 229E associated with acute upper respiratory tract symptoms in Kuala Lumpur, Malaysia. *Am J Trop Med Hyg 94:* 1058–1064.</jrn>

<jrn>18. Risku M, Lappalainen S, Rasanen S, Vesikari T, 2010. Detection of human coronaviruses in children with acute gastroenteritis. *J Clin Virol 48:* 27–30.</jrn>

<jrn>19. Lednicky JA, Waltzek TB, McGeehan E, Loeb JC, Hamilton SB, Luetke MC, 2013. Isolation and genetic characterization of human coronavirus NL63 in primary human renal proximal tubular epithelial cells obtained from a commercial supplier, and confirmation of its replication in two different types of human primary kidney cells. *Virol J 10:* 213.</jrn>

<jrn>20. Cowling BJ, Park M, Fang VJ, Wu P, Leung GM, Wu JT, 2015. Preliminary epidemiological assessment of MERS-CoV outbreak in South Korea, May to June 2015. *Euro Surveill 20:* 21163.</jrn>

FIGURE 1. LLC-MK2 cells. Noninoculated cells (**A**) appear crowded 13 days postseed; no spaces are present between the cells and the nuclei have prominent nucleoli. (**B**) Cells 13 days postinoculation with plasma sample four appear different: the nuclei of the infected cells appear larger, lack prominent nucleoli, and have visibly darker nuclear borders (black arrows), and clearings due to detachment of dead cells are evident, as are a few refractile floating dead cells. The virus grew at both 33°C and 37°C; this figure shows virus in cells grown at 33°C. The appearance of the nuclei of the infected LLC-MK2 cells is consistent with HCoV-NL63 infections. Localization to the nucleolus is a common feature of coronavirus nucleoproteins, resulting in the accumulation of cells in the M-phase of the cell cycle (nucleoli are absent in dividing cells), and the formation in syncytia in a fraction of the cells. Moreover, immature HCoV-NL63 particles form in the RER surrounding the nucleus, and the dark border surrounding the enlarged nuclei in Figure 1B are likely due to cellular changes in the RER of the infected cells. Representative photomicrographs of cytopathic effects of other viral species are shown in Supplemental Figures 2—4. This figure appears in color at www.ajtmh.org.

FIGURE 2. Maximum Clade Credibility tree of HCoV-NL63 spike gene region. Branches are colored according to the legend to the left where each color represents the geographic location of the sampled sequence (tip branches), as well as of the ancestral lineage (internal branches) inferred by Bayesian phylogeography. The tree was scaled in time by enforcing a relaxed molecular clock (see Supplemental Information). One asterisk along the branch represents significant statistical support (posterior probability ≥ 90%). Sequence labels for the new strains are shown. This figure appears in color at www.ajtmh.org.

Viral culture, identification, and sequencing.

Cell cultures.

Cell lines A549 (CCL-185), LLC-MK2 (CCL-7), MDCK, (CCL-34), MRC5, and Vero E6 (CRL-1586) were obtained from the American Type Culture Collection (Manassas, VA), and were propagated as monolayers at 37°C and 5% CO_2 in Advanced Dulbecco's Modified Eagle's Medium (aDMEM) (Invitrogen Corp., Carlsbad, CA) or Eagle's Minimal Essential Medium (EMEM) (Invitrogen Corp.), as appropriate per cell line. aDMEM and EMEM were supplemented with 2 mM L-Alanyl-L-Glutamine (GlutaMAX™; Invitrogen Corp.), antibiotics (PSN; 50 μg/mL penicillin, 50 μg/mL streptomycin, 100 μg/mL neomycin [Invitrogen Corp.]), and 10% (v/v) low IgG, heat-inactivated gamma-irradiated fetal bovine serum (FBS) (HyClone, Logan, UT). Additionally, sodium pyruvate (Invitrogen Corp.) and nonessential amino acids (HyClone) were added to EMEM. Before seed stocks were prepared, the cell lines were propagated in growth media with plasmocin (Invivogen, San Diego, CA) for 2 weeks to reduce the chances of mycoplasma contamination, then for a minimum of 2 weeks in the absence of antibiotics to determine whether fast-growing microbial contaminants were present or abnormal morphological changes would occur (associated with intracellular mycoplasma). Following 2–3 weeks of propagation without antibiotics, the plasmocin-treated cell lines were tested by polymerase chain reaction (PCR) to confirm an absence of mycoplasma DNA.[1]

Virus isolation.

Aliquots of plasma (25–100 μL) from febrile patients that had tested negative for Chikungunya virus RNA by reverse transcription PCR (RT-PCR) (details to be presented elsewhere) were inoculated onto duplicate sets of cells grown in 25 cm^2 rectangular canted-neck cell culture flasks with vent caps (Cat no. 430639, Corning Incorporated, Corning, NY). A total of 10 flasks were used per plasma sample. Cell culture flasks were used so that plasma could be inoculated onto a relatively wide surface area; otherwise, the complex mix of biomolecules in human plasma/serum can induce nonspecific cytopathic effects (CPEs) that are mistaken for virus-induced CPE. Sets consisting of five different cell lines (A549, LLC-MK2, MDCK, MRC5, and Vero E6) were used to increase the chance of isolating a wide array of viruses. One set was inoculated at 37°C, the other at 33°C. All cells were in complete medium with serum, except for MDCK cells at 33°C, which were in serum-free medium containing 2 μg/mL of L-1-tosylamide-2-phenylethyl chloromethyl ketone (TPCK)-treated trypsin.[2] Noninoculated cells were held in parallel with the inoculated cells and served as negative controls. All the cells were observed daily for development of virus-induced CPE using an inverted microscope with phase-contrast optics, and refed every 3 days with complete medium containing either 4% FBS (or serum-free medium with TPCK trypsin). The cells were maintained and observed for 1 month before being considered negative for virus isolation.

Virus screens.

This work was focused on the isolation and/or detection of alpha- and flaviviruses, and PCR-based methods for the detection of the nucleic acids of those viruses (to be presented elsewhere) were used for primary screens. A limited number of PCR-based methods were also used for secondary tests; these were for the detection of arenaviruses and enteroviruses, which are viruses

that could be in serum/plasma in febrile patients. Furthermore, the GenMark multiplex respiratory PCR eSensor XT-8 Respiratory Viral Panel (eSensor RVP; GenMark Diagnostics, Inc., Carlsbad, CA) was used to screen for respiratory viruses according to instructions from the manufacturer. The system detects the genomic material of influenza A virus (including subtypes H1 and H3), influenza A virus 2009 H1N1, influenza B virus, respiratory syncytial viruses A and B, parainfluenza viruses 1, 2, 3, and 4, human metapneumovirus, adenoviruses B/E and C, human coronaviruses (HCoVs) (-229E, -NL63, -HKU1, -OC43), and human rhinoviruses A and B. Briefly, in the case of viral genomic RNA (vRNA), the extracted nucleic acid is reverse transcribed and amplified using viral-specific primers with an RT-PCR enzyme mix. The amplified DNA is converted to single-stranded DNA via exonuclease digestion and is combined with a signal buffer containing ferrocene-labeled signal probes that are specific for the different viral targets. A signal in nanoAmperes (nA) is provided; signals higher than a threshold value are considered positive.

RT-PCR tests for confirmation of HCoV-NL63.

Following detection of HCoV-NL63 vRNA by the GenMark eSensor XT-8 RVP, confirmation was attained using methods outlined in reference.[3] Briefly, vRNA was extracted from spent cell media using a QIAamp Viral RNA kit (QIAGEN, Valencia, CA), and RT-PCR amplicons generated using primer pairs Cor-FW and Cor-RV,[4] N5-PCR1 and N3-PCR1,[4] and repSZ-1 and repSZ-3,[5] were sequenced. Reverse transcription procedures were performed with Omniscript reverse transcriptase (Qiagen), and PCR with Hotshot TAQ (New England Biolabs, Ipswich, MA) with extension at 68°C.

Nucleotide sequencing.

Targeted HCoV-NL63 sequences were RT-PCR-amplified from purified vRNA using a genome walking strategy (3). Briefly, overlapping primers described by Geng and others (GenBank JX524171) and others[4,5] were used to obtain the complete genomic sequence of one of the HCoV-NL63 isolates from Haiti (designated HCoV-NL63/Haiti-1/2015). Following the same methods, spike, membrane, and nucleocapsid gene sequences were also obtained for HCoV-NL63 isolates 2, 3, and 4 from Hiati. As before,[3] AccuScript High Fidelity Reverse Transcriptase (Agilent Technologies Inc., Santa Clara, CA) was used for first-strand cDNA synthesis in the presence of SUPERase-In RNase inhibitor (Ambion, Austin, TX), and PCR was performed using Phusion Polymerase (New England Biolabs) with denaturation steps performed at 98°C. The 3′ and 5′ ends of HCoV-NL63/Haiti-1/2015 were determined using a RACE (rapid amplification of cDNA ends) kit (RLM RACE; Ambion) following the manufacturer's instructions. For all, nucleotide sequences were analyzed using an Applied Biosystem 3130 DNA analyzer by using BigDye Terminator (v. 3.1) chemistry and the same primers used for amplifications.

GenBank accession numbers.

HCoV-NL63/Haiti: KT266906; KX179494- KX179499. HCoV-NL63/Florida: KT381875.1; KU521535.1

Phylogenetic analysis.

Forty-four complete genome and 148 spike gene region sequences were downloaded from NCBI (Supplemental Table 1). Inclusion criteria for the sequences were 1) the sequences were

published in peer-reviewed journals, 2) no uncertainty regarding the subtype assignment and being classified, 3) potential recombinants or poor-quality sequences (i.e., sequences with uncertain nucleotide assignments) were excluded, and 4) city/state and sampling time were known and clearly established in the original publication. The locations of the reference sequences considered for the analysis were Belgium, China, Ghana, Hong Kong, Japan, Malaysia, the Netherlands, Sweden, Thailand, and the United States. A multiple sequence alignment of the spike gene region, including the 192 references sequences as well as the two new sequences from Shands and the four from Haiti, was then obtained with ClustalX[6] followed by manual editing using Bioedit.[7] The evolutionary model was chosen as the best-fitting nucleotide substitution model in accordance with the results of the hierarchical likelihood ratio test implemented with the Modeltest software version 3.7.[8] The full alignment is available from the authors on request.

Likelihood mapping and phylogenetic inference.

The phylogenetic signal in the aligned sequences was investigated with the likelihood mapping method that analyzes every possible group of four sequences, referred to as a "quartet."[9] For each quartet, the likelihood of each one of the three possible unrooted trees is estimated, and the three likelihoods are eventually reported as a dot in an equilateral triangle (the likelihood map) that is subdivided in to three main areas: the three corners, representing fully resolved tree topologies (i.e., the presence of treelike phylogenetic signal in the data); the center, representing star-like phylogeny signal (i.e., phylogenetic noise); and the three side areas indicating network-like phylogeny (i.e., presence of recombination or conflicting phylogenetic signals). Findings from extensive simulation studies suggest that a central area with < 30% dots can be used as the criterion of robust phylogenetic signal. The likelihood mapping analysis was performed with the program TREE-PUZZLE.[9] The percentage of dots (noise level) falling in the central likelihood map was 15.5% indicating sufficient signal to infer a robust phylogeny.

Bayesian time-scaled phylogeny.

The evolutionary rate of the Coronavirus NL63 spike region was estimated by calibrating a molecular clock using known sequences sampling times with the Bayesian Markov Chain Monte Carlo (MCMC) method implemented in BEAST v. 1.8 (http://beast.bio.ed.ac.uk) [10,11] and by enforcing either a strict or a relaxed molecular clock with an lognormal distribution for the prior rates. Four independent MCMC runs were carried out enforcing a relaxed molecular clock (which resulted the best fit for the data, see Results Section) and one of the following coalescent priors: constant population size, exponential growth, nonparametric smooth skyride plot Gaussian Markov random field, and nonparametric Bayesian skyline plot.[10,12,13] Marginal likelihoods estimates for each model were obtained using path sampling and stepping stone analyses.[14–16] Uncertainty in the estimates was indicated by 95% high posterior density intervals, and the best fitting model for the data set was selected by calculating the Bayes factors (BFs).[15,17] In practice, any two models were compared to evaluate the strength of evidence against the null hypothesis (H_0), defined as the one with the lower marginal likelihood: $2ln\text{BF} < 2$ indicates no evidence against H_0; 2–6, weak evidence; 6–10, strong evidence; and > 10 very strong evidence. For each data set, the MCMC sampler was run for at least 50×10^6 generations, sampling every 5,000 generations. Proper mixing of the MCMC was assessed by calculating the effective sample size (ESS) of each parameter. Only parameter estimates with ESS > 250 were accepted. Phylogeographic analysis was conducted by using the continuous time Markov chain process

over discrete sampling locations implemented in BEAST[18] with the Bayesian Stochastic Search Variable Selection model, which allows diffusion rates to be zero with a positive prior probability. The maximum clade credibility tree was selected from the posterior tree distribution after a 10% burn-in using Tree Annotator version 1.8 included in the BEAST package.[10,11] Statistical support for specific monophyletic clades was assessed by calculating the posterior probability. The phylogenetic tree with full sequence labels is included in Supplemental Figure 1.

REFERENCES

<edb>1. Lednicky JA, Wyatt DE, 2012. The art of animal cell culture for virus isolation. Ceccherini-Nell L, Zagreb MB, eds. *Biomedical Tissue Culture*. Croatia: InTech, 151–178. ISBN 978–953–51.</edb>

<jrn>2. Hamilton SB, Wyatt DE, Wahlgren BT, O'Dowd MK, Morrissey JM, Daniels DE, Lednicky JA, 2011. Higher titers of some H5N1 and recent human H1N1 and H3N2 influenza viruses in Mv1 Lu vs. MDCK cells. *Virol J 8:* 66.</jrn>

<jrn>3. Lednicky JA, Waltzek TB, McGeehan E, Loeb JC, Hamilton SB, Luetke MC, 2013. Isolation and genetic characterization of human coronavirus NL63 in primary human renal proximal tubular epithelial cells obtained from a commercial supplier, and confirmation of its replication in two different types of human primary kidney cells. *Virol J 10:* 213.</jrn>

<jrn>4. Moës E, Vijgen L, Keyaerts E, Zlateva K, Li S, Maes P, Pyrc K, Berkhout B, van der Hoek L, van Ranst M, 2005. A novel pancoronavirus RT-PCR assay: frequent detection of human coronavirus NL63 in children hospitalized with respiratory tract infections in Belgium. *BMC Infect Dis 5:* 6.</jrn>

<jrn>5. van der Hoek L, Pyrc K, Jebbink MF, Vermeulen-Oost W, Berkhout RJ, Wolthers KC, Wertheim-van Dillen PM, Kaandorp J, Spaargaren J, Berkhout B, 2004. Identification of a new human coronavirus. *Nat Med 10:* 368–373.</jrn>

<jrn>6. Thompson JD, Gibson TJ, Plewniak F, Jeanmougin F, Higgins DG, 1997. The CLUSTAL_X windows interface: flexible strategies for multiple sequence alignment aided by quality analysis tools. *Nucleic Acids Res 25:* 4876–4882.</jrn>

<jrn>7. Hall TA. 1999. BioEdit: a user-friendly biological sequence alignment editor and analysis program for Windows 95/98/NT. *Nucleic Acids Symp 41:* 95–98.</jrn>

<jrn>8. Posada D, Buckley TR, 2004. Model selection and model averaging in phylogenetics: advantages of akaike information criterion and bayesian approaches over likelihood ratio tests. *Syst Biol 53:* 793–808.</jrn>

<jrn>9. Schmidt HA, Strimmer K, Vingron M, von Haeseler A, 2002. TREE-PUZZLE: maximum likelihood phylogenetic analysis using quartets and parallel computing. *Bioinformatics 18:* 502–504.</jrn>

<jrn>10. Drummond AJ, Rambaut A, Shapiro B, Pybus OG, 2005. Bayesian coalescent inference of past population dynamics from molecular sequences. *Mol Biol Evol 22:* 1185–1192.</jrn>

<jrn>11. Drummond AJ, Rambaut A, 2007. BEAST: Bayesian evolutionary analysis by sampling trees. *BMC Evol Biol 7:* 214.</jrn>

<jrn>12. Drummond AJ, Nicholls GK, Rodrigo AG, Solomon W, 2002. Estimating mutation parameters, population history and genealogy simultaneously from temporally spaced sequence data. *Genetics 61:* 1307–1320.</jrn>

<jrn>13. Minin VN, Bloomquist EW, Suchard MA, 2008. Smooth skyride through a rough skyline: Bayesian coalescent-based inference of population dynamics. *Mol Biol Evol 25:* 1459–1471.</jrn>

<jrn>14. Baele G, Lemey P, Vansteelandt S, 2013. Make the most of your samples: Bayes factor estimators for high-dimensional models of sequence evolution. *BMC Bioinformatics 14:* 85.</jrn>

<jrn>15. Baele G, Li WLS, Drummond AJ, Suchard MA, Lemey P, 2013. Accurate model selection of relaxed molecular clocks in bayesian phylogenetics. *Mol Biol Evol 30:* 239–243.</jrn>

<jrn>16. Baele G, Lemey P, 2013. Bayesian evolutionary model testing in the phylogenomics era: matching model complexity with computational efficiency. *Bioinformatics 29:* 1970–1979.</jrn>

<jrn>17. Kass RE, Raftery AE, 1995. Bayes factors. *J Am Stat Assoc 90:* 773–795.</jrn>

<jrn>18. Lemey P, Rambaut A, Drummond AJ, Suchard MA, 2009. Bayesian phylogeography finds its roots. *PLOS Comput Biol 5:* 1–16.</jrn>

SUPPLEMENTAL FIGURE 1. Maximum Clade Credibility (MCC) tree of HCoV-NL63 spike gene region with sequence labels. Branches are colored according to the legend in Figure 2, where each color represents the geographic location of the sampled sequence (tip branches), as well as of the ancestral lineage (internal branches) inferred by Bayesian phylogeography. For display purposes, the tree is displayed as a polar tree.

SUPPLEMENTAL FIGURE 2. *Enterovirus* D68 in A549 cells. (**A**) Mock-infected A549 cells, 6 days post-seed. (**B**) A549 cells, 6 days postinoculation with plasma. Infected cells display characteristic cytopathic effect (CPE) at 33°C: cell rounding followed by detachment from the growing surface, whereas CPE are not observed at 37°C (not shown). Images at an original magnification at ×200.

SUPPLEMENTAL FIGURE 3. Dengue viruses in Vero E6 cells incubated at 37°C. (**A**) Mock-infected Vero cells, 8 days postseed. (**B**) *Dengue virus* 1- infected cells, 8 days postinoculation with plasma. (**C**) *Dengue virus* 4-infected cells, 8 days postinoculation with plasma. The virus infected cells display diffuse cytopathic effect (CPE) including darkening of the cytoplasm prior to death (colorless refractile cells). Some infected cells contain one or more large vacuoles. Images at an original magnification of ×200.

SUPPLEMENTAL FIGURE 4. Zika virus in LLC-MK2 cells. (**A**) Mock-infected LLC-MK2 cells, 9 days post-seed, image at original magnification ×200. (**B**) *Zika virus*-infected cells, 9 days post-inoculation with plasma, image at original magnification 200X. (**C**) Mock-infected LLC-MK2 cells, 9 days post-seed, image at original magnification ×400. (**D**) *Zika virus*-infected cells, 9 days post-inoculation with plasma, image at original magnification ×400. Prior to cell death, perinuclear vacuoles are present in most cells (white arrows).

SUPPLEMENTAL TABLE 1

Accession number, gene region and country of reference sequences included in this study

Accession number	Gene region	Country	Tip name
KT381875	Complete genome	United States	Shands
KU521535	Complete genome	United States	SHANDS_2
KT266906	Complete genome	Haiti	HAITI1
JX504050	Complete genome	United States	2US04
JX104161	Complete genome	China	3CN08
AB695189	Spike glycoprotein	Japan	4JP11
AB695188	Spike glycoprotein	Japan	5JP11
AB695187	Spike glycoprotein	Japan	6JP10
AB695186	Spike glycoprotein	Japan	7JP10
AB695185	Spike glycoprotein	Japan	8JP10
AB695184	Spike glycoprotein	Japan	9JP10
AB695183	Spike glycoprotein	Japan	10JP10
DQ462792	Spike glycoprotein	Netherlands	11NL03
DQ462789	Spike glycoprotein	Netherlands	14NL03
DQ462788	Spike glycoprotein	Netherlands	15NL03
DQ462787	Spike glycoprotein	Netherlands	16NL03
DQ462786	Spike glycoprotein	Netherlands	17NL03
DQ462785	Spike glycoprotein	Netherlands	18NL03
DQ462784	Spike glycoprotein	Netherlands	19NL04
DQ462783	Spike glycoprotein	Netherlands	20NL04
DQ462782	Spike glycoprotein	Netherlands	21NL02
AY758299	Spike glycoprotein	Belgium	23BE03
AY758301	Spike glycoprotein	Belgium	24BE03
AY758300	Spike glycoprotein	Belgium	25BE03
AY758298	Spike glycoprotein	Belgium	26BE03
AY758297	Spike glycoprotein	Belgium	27BE03
GQ856814	Spike glycoprotein	Hong Kong	29HK05
GQ856812	Spike glycoprotein	Hong Kong	30HK05
GQ856813	Spike glycoprotein	Hong Kong	31HK05
GQ856811	Spike glycoprotein	Hong Kong	32HK05
GQ856810	Spike glycoprotein	Hong Kong	33HK05
GQ856809	Spike glycoprotein	Hong Kong	34HK06
GQ856808	Spike glycoprotein	Hong Kong	35HK06
GQ856807	Spike glycoprotein	Hong Kong	36HK06
GQ856806	Spike glycoprotein	Hong Kong	37HK06
GQ856805	Spike glycoprotein	Hong Kong	38HK06
GQ856804	Spike glycoprotein	Hong Kong	39HK06
GQ856803	Spike glycoprotein	Hong Kong	40HK06
GQ856802	Spike glycoprotein	Hong Kong	41HK06
GQ856801	Spike glycoprotein	Hong Kong	42HK06
GQ856800	Spike glycoprotein	Hong Kong	43HK06
GQ856799	Spike glycoprotein	Hong Kong	44HK06
GQ856798	Spike glycoprotein	Hong Kong	45HK06
DQ445912	Complete genome	Netherlands	52NL03
DQ445911	Complete genome	Netherlands	53NL04
DQ231166	Spike glycoprotein	Sweden	54SE04
DQ231165	Spike glycoprotein	Sweden	55SE05
DQ231164	Spike glycoprotein	Sweden	56SE05
DQ231163	Spike glycoprotein	Sweden	57SE05

DQ231162	Spike glycoprotein	Sweden	58SE05
DQ231161	Spike glycoprotein	Sweden	59SE04
DQ231160	Spike glycoprotein	Sweden	60SE04
DQ231159	Spike glycoprotein	Sweden	61SE04
DQ231158	Spike glycoprotein	Sweden	62SE05
AY902242	Spike glycoprotein	Sweden	63SE04
NC_005831	Complete genome	Netherlands	64NL03
AY567487	Complete genome	Netherlands	65NL03
KT359913	Spike glycoprotein	Malaysia	66MY13
KT359912	Spike glycoprotein	Malaysia	67MY13
KT359911	Spike glycoprotein	Malaysia	68MY13
KT359910	Spike glycoprotein	Malaysia	69MY13
KT359909	Spike glycoprotein	Malaysia	70MY12
KT359908	Spike glycoprotein	Malaysia	71MY12
KT359907	Spike glycoprotein	Malaysia	72MY12
KT359906	Spike glycoprotein	Malaysia	73MY12
KT359905	Spike glycoprotein	Malaysia	74MY12
KT359904	Spike glycoprotein	Malaysia	75MY12
KT359903	Spike glycoprotein	Malaysia	76MY12
KT359902	Spike glycoprotein	Malaysia	77MY12
KT359901	Spike glycoprotein	Malaysia	78MY12
KT359900	Spike glycoprotein	Malaysia	79MY12
KT359899	Spike glycoprotein	Malaysia	80MY12
KT359898	Spike glycoprotein	Malaysia	81MY12
KT359897	Spike glycoprotein	Malaysia	82MY12
KT359896	Spike glycoprotein	Malaysia	83MY12
KT359895	Spike glycoprotein	Malaysia	84MY12
KT359894	Spike glycoprotein	Malaysia	85MY12
KT359893	Spike glycoprotein	Malaysia	86MY12
KT359892	Spike glycoprotein	Malaysia	87MY12
KT359891	Spike glycoprotein	Malaysia	88MY12
KT359890	Spike glycoprotein	Malaysia	89MY12
KT359889	Spike glycoprotein	Malaysia	90MY12
KT359888	Spike glycoprotein	Malaysia	91MY12
KT359887	Spike glycoprotein	Malaysia	92MY12
KT359886	Spike glycoprotein	Malaysia	93MY12
KT359885	Spike glycoprotein	Malaysia	94MY12
KT359884	Spike glycoprotein	Malaysia	95MY12
KT359883	Spike glycoprotein	Malaysia	96MY12
KT359882	Spike glycoprotein	Malaysia	97MY12
KT359881	Spike glycoprotein	Malaysia	98MY12
KT359880	Spike glycoprotein	Malaysia	99MY12
KT359879	Spike glycoprotein	Malaysia	100MY12
KT359878	Spike glycoprotein	Malaysia	101MY12
KT359877	Spike glycoprotein	Malaysia	102MY12
KT359876	Spike glycoprotein	Malaysia	103MY12
KT359875	Spike glycoprotein	Malaysia	104MY12
KT359874	Spike glycoprotein	Malaysia	105MY12
KT359873	Spike glycoprotein	Malaysia	106MY12
KT359872	Spike glycoprotein	Malaysia	107MY12
KM077093	Spike glycoprotein	United States	108US91
KM077092	Spike glycoprotein	United States	109US93
KM077091	Spike glycoprotein	United States	110US95

KM077090	Spike glycoprotein	United States	111US97
KM077089	Spike glycoprotein	United States	112US01
KM077088	Spike glycoprotein	United States	113US83
KM077087	Spike glycoprotein	United States	114US87
KM077086	Spike glycoprotein	United States	115US92
KM077085	Spike glycoprotein	United States	116US90
KM077084	Spike glycoprotein	United States	117US89
KM077083	Spike glycoprotein	United States	118US90
KM077082	Spike glycoprotein	United States	119US89
KM077081	Spike glycoprotein	United States	120US90
KM077080	Spike glycoprotein	United States	121US90
KM077079	Spike glycoprotein	United States	122US99
KM077078	Spike glycoprotein	United States	123US01
KM077077	Spike glycoprotein	United States	124US91
KM077076	Spike glycoprotein	United States	125US96
KM077075	Spike glycoprotein	United States	126US96
KM077074	Spike glycoprotein	United States	127US93
KM077073	Spike glycoprotein	United States	128US92
KM077072	Spike glycoprotein	United States	129US91
KF530114	Complete genome	United States	130US89
KF530113	Complete genome	United States	131US90
KF530112	Complete genome	United States	132US01
KF530111	Complete genome	United States	133US90
KF530110	Complete genome	United States	134US83
KF530109	Complete genome	United States	135US90
KF530108	Complete genome	United States	136US89
KF530107	Complete genome	United States	137US91
KF530106	Complete genome	United States	138US87
KF530105	Complete genome	United States	139US01
KF530104	Complete genome	United States	140US90
JQ900259	Complete genome	United States	142US05
JQ900257	Complete genome	United States	144US09
JQ900256	Complete genome	United States	145US09
JQ900255	Complete genome	United States	146US09
JQ765575	Complete genome	United States	147US05
JQ765574	Complete genome	United States	148US05
JQ765573	Complete genome	United States	149US05
JQ765572	Complete genome	United States	150US05
JQ765571	Complete genome	United States	151US05
JQ765570	Complete genome	United States	152US05
JQ765569	Complete genome	United States	153US05
JQ765568	Complete genome	United States	154US05
JQ765567	Complete genome	United States	155US09
JQ765566	Complete genome	United States	156US08
JQ765565	Complete genome	United States	157US09
JQ765564	Complete genome	United States	158US09
JQ765563	Complete genome	United States	159US09
JQ771060	Complete genome	United States	160US10
JQ771059	Complete genome	United States	161US10
JQ771058	Complete genome	United States	162US10
JQ771057	Complete genome	United States	163US10
JQ771056	Complete genome	United States	164US10
JQ771055	Complete genome	United States	165US10

KJ796467	Spike glycoprotein	Ghana	166GH12
KJ796466	Spike glycoprotein	Ghana	167GH12
KJ796465	Spike glycoprotein	Ghana	168GH12
KJ768643	Spike glycoprotein	Ghana	169GH12
KJ768642	Spike glycoprotein	Ghana	170GH12
KJ768641	Spike glycoprotein	Ghana	171GH12
KJ768640	Spike glycoprotein	Ghana	172GH12
KJ768639	Spike glycoprotein	Ghana	173GH12
KJ768638	Spike glycoprotein	Ghana	174GH12
KJ768637	Spike glycoprotein	Ghana	175GH12
KJ768636	Spike glycoprotein	Ghana	176GH12
KJ768635	Spike glycoprotein	Ghana	177GH12
KJ768634	Spike glycoprotein	Ghana	178GH12
KJ768633	Spike glycoprotein	Ghana	179GH12
JX513255	Spike glycoprotein	Thailand	180TH10
JX513253	Spike glycoprotein	Thailand	181TH10
JX513249	Spike glycoprotein	Thailand	182TH10
JX524171	Complete genome	China	183CN09
FJ656174	Spike glycoprotein	Sweden	184SE07
FJ656173	Spike glycoprotein	Sweden	185SE07
FJ656172	Spike glycoprotein	Sweden	186SE07
FJ656171	Spike glycoprotein	Sweden	187SE07
FJ656170	Spike glycoprotein	Sweden	188SE07
FJ656169	Spike glycoprotein	Sweden	189SE07
FJ656168	Spike glycoprotein	Sweden	190SE06
FJ656167	Spike glycoprotein	Sweden	191SE07
FJ656166	Spike glycoprotein	Sweden	192SE07
FJ656165	Spike glycoprotein	Sweden	193SE07
FJ656164	Spike glycoprotein	Sweden	194SE07
FJ656163	Spike glycoprotein	Sweden	195SE07
FJ656162	Spike glycoprotein	Sweden	196SE07
FJ656161	Spike glycoprotein	Sweden	197SE07
FJ656160	Spike glycoprotein	Sweden	198SE07
FJ656159	Spike glycoprotein	Sweden	199SE07
FJ656158	Spike glycoprotein	Sweden	200SE07
FJ656157	Spike glycoprotein	Sweden	201SE07
FJ656156	Spike glycoprotein	Sweden	202SE06
FJ656155	Spike glycoprotein	Sweden	203SE06
FJ656154	Spike glycoprotein	Sweden	204SE06
FJ656153	Spike glycoprotein	Sweden	205SE06

Figure 1

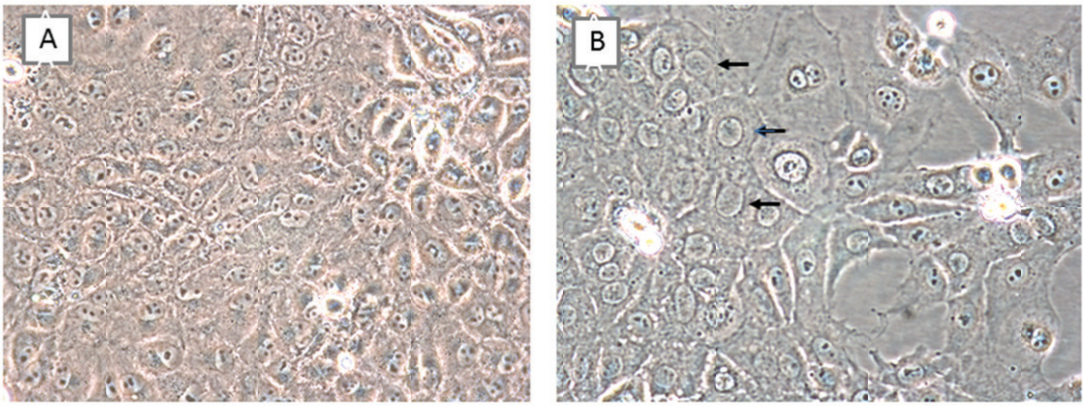

Figure 2

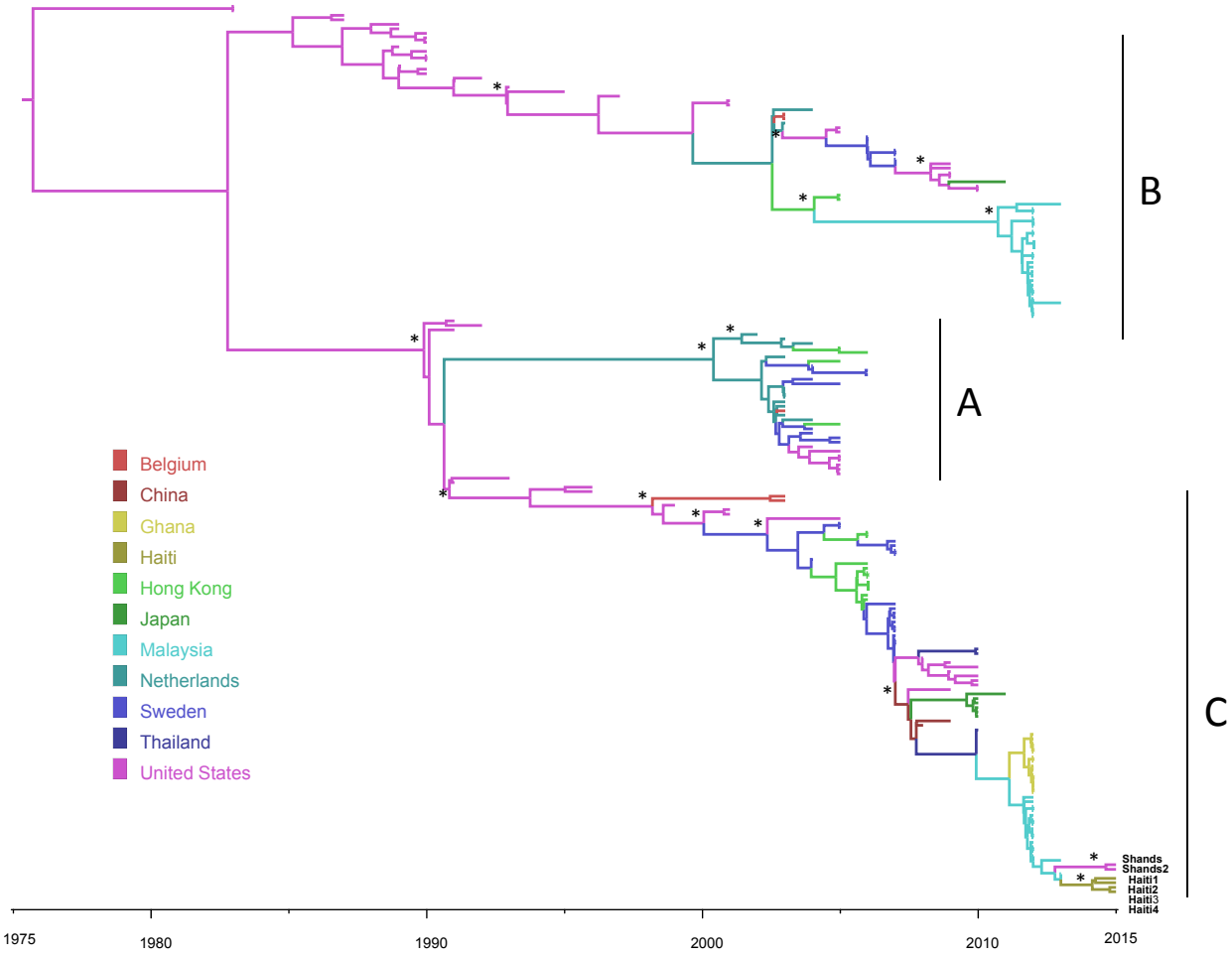
B
A
C
Belgium
China
Ghana
Haiti
Hong Kong
Japan
Malaysia
Netherlands
Sweden
Thailand
United States
Shands
Shands2
Haiti1
Haiti2
Haiti3
Haiti4
1975
1980
1990
2000
2010
2015

Supplementary Figure 1

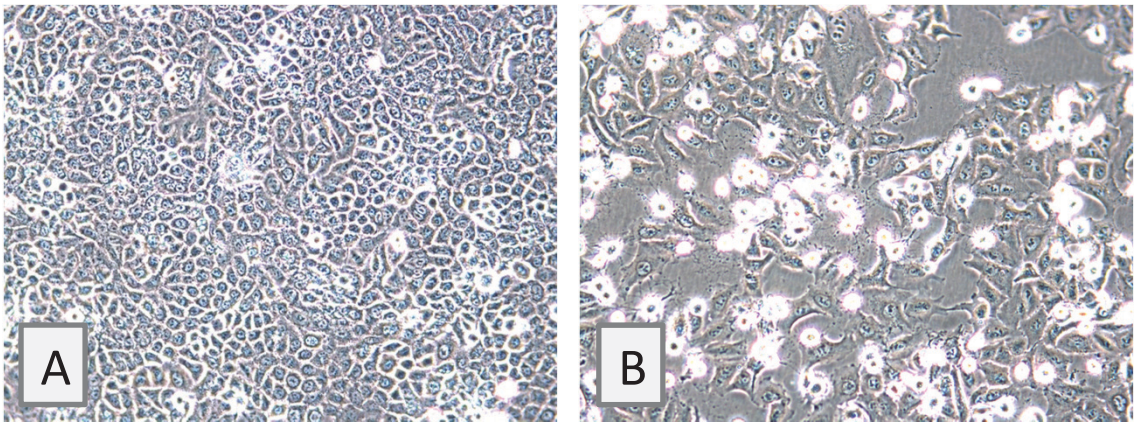

Supplementary Figure 2

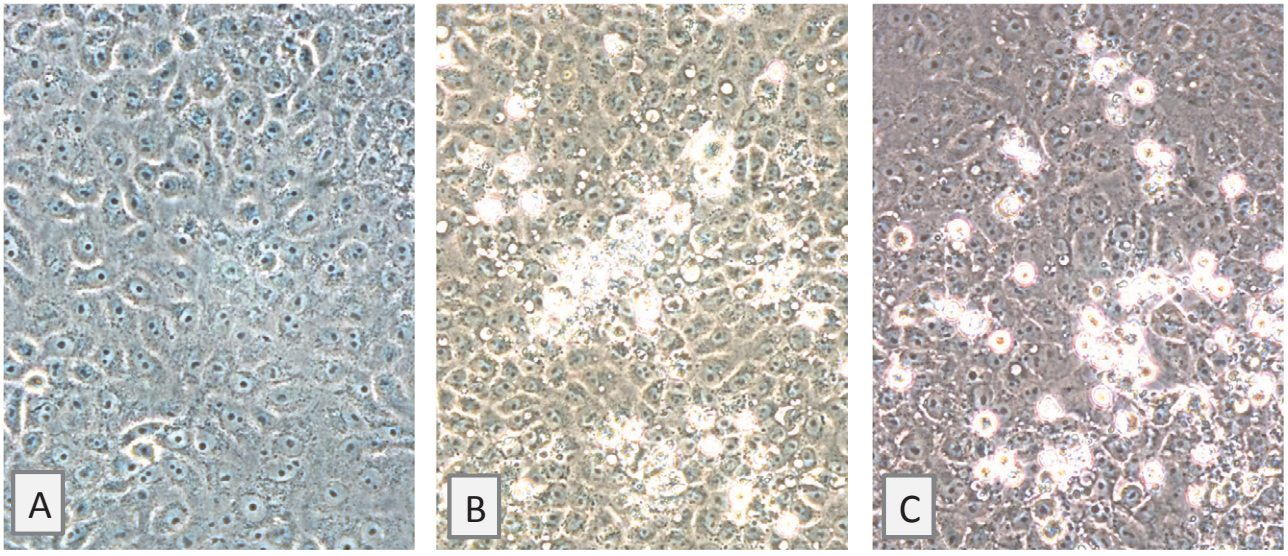

Supplementary Figure 3

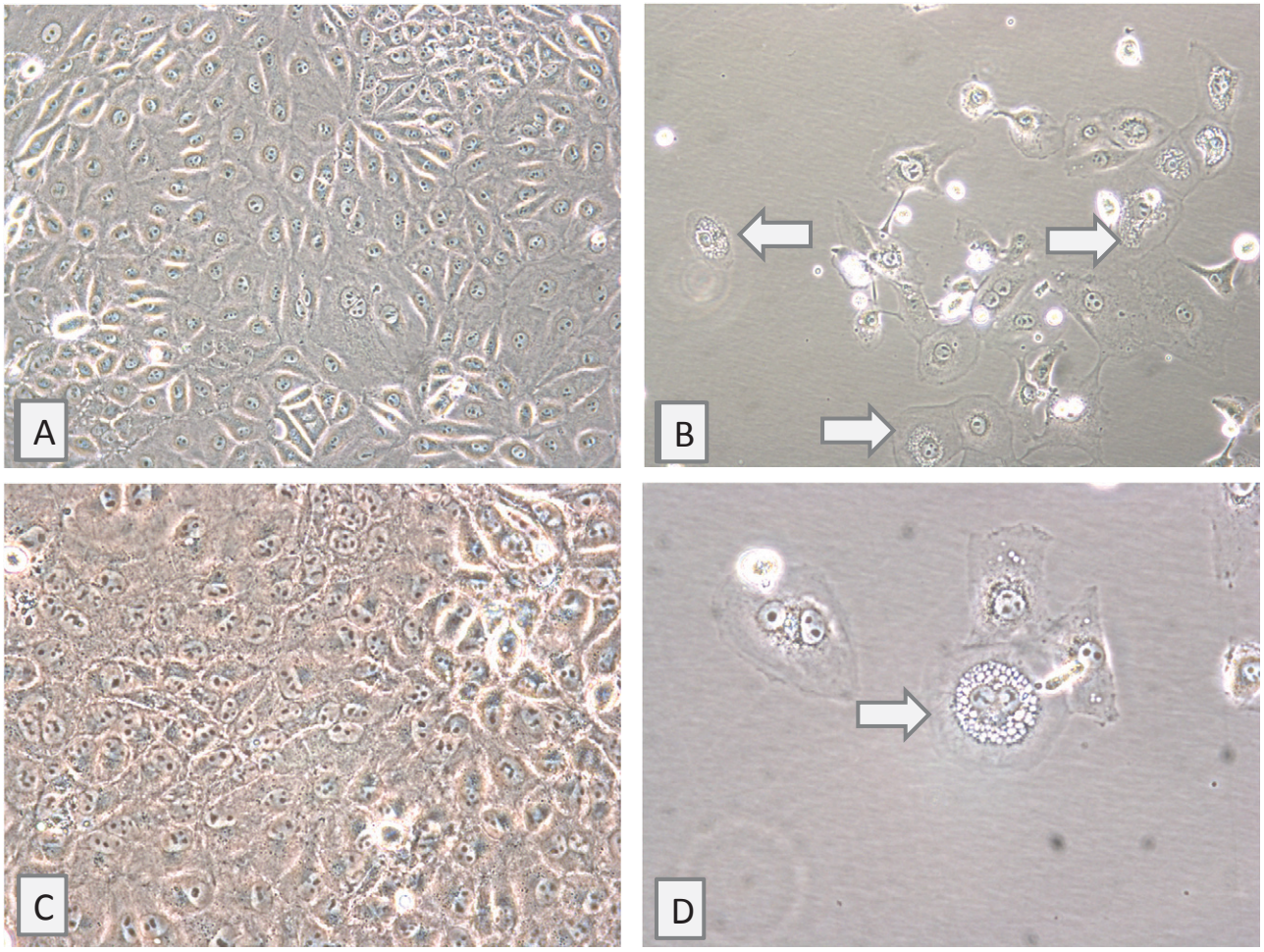

Supplementary Figure 4